TECHNICAL PAPER

Micro harvester using isotropic charging of electrets deposited on vertical sidewalls for conversion of 3D vibrational energy

Ulrich Mescheder · Antwi Nimo · Bernhard Müller ·
Awad Saad Abou Elkeir

Abstract The design and fabrication process of an integrated micro energy harvester capable of harvesting electrical energy from low amplitude mechanical vibrations is presented. A specific feature of the presented energy harvester design is its capability to harvest vibrational energy from different directions (3D). This is done through an innovative approach of electrets placed on vertical sidewalls, allowing miniaturization of 3D capacitive energy harvester fabrication on monolithic CMOS substrates. A new simple electret charging method using ionic hair-dryers is used. The charging performance of SiO_2 and CYTOP electrets are characterized for electrets in horizontal arrangement and electrets deposited on vertical sidewalls.

1 Introduction

1.1 Motivation

Batteries still play the major role in powering remote low power autonomous systems even though obvious disadvantages such as overall system's size increase due to batteries and limited battery lifetime makes them inconvenient

U. Mescheder (✉) · A. Nimo · B. Müller · A. S. A. Elkeir
Department Electrical and Computer Engineering/Institute
for Applied Research, Furtwangen University,
Robert-Gerwig-Platz 1, 78120 Furtwangen, Germany
e-mail: mes@hs-furtwangen.de

A. Nimo
e-mail: antwi.nimo@imtek.de

Present Address:
A. Nimo
IMTEK-Institut für Mikrosystemtechnik,
79110 Freiburg, Germnay

e.g. for remote low power sensor nodes. This setback of batteries has boosted research into alternative renewable sources of powering remote low power systems such as Si-based microsystems (e.g. gyros, accelerometers etc.). For such systems, harvesters supplying power in the range of microwatt to milliwatt and capable of been integrated monolithically into microsystems might allow for realization of autonomous miniaturized systems. This work seeks to design and fabricate an integrated micro energy harvester capable of harvesting electrical energy from low amplitude (1 g) and multi-axial mechanical vibrations. Additionally, designs and fabrication compatible with standard CMOS processing have enormous advantages in batch processes for mass production without the need to bring separate components together. Cheap and simple charging method for electret is investigated to demonstrate its use in electret-based micro energy harvesters.

1.2 State of art

An early approach of harvesting vibrational energy from the environment by a spring-mass-system and by electromagnetic energy conversion was presented by Williams and Yates (1996). Since then different types of harvesters using other conversion techniques like piezoelectric, thermoelectric, electrochemical, electro-static and by inductive/capacitive coupling methods from energy sources like vibration, heat, light (waves) or chemicals have been investigated. There is a general consensus that these renewable methods of powering low power systems will be used in future remote low power sensor nodes. Low power sensor nodes will require sources of power that are renewable and harvesters that are small enough to be able to replace batteries. Design complications in the micro range and scaling effects of power output as device dimensions reach the micro range, make electrostatic vibration

micro harvesting dominant compared to other techniques. Electrostatic vibration micro-harvesters provide CMOS compatible realization. Electret-based vibration energy harvesters have been reported by Tsutsumino et al. (2006) and Edamoto et al. (2006, 2009), using high performance electrets to bias comb-like capacitors to realize electrostatic vibration micro-harvesters, which can harvest energy at a specific frequency and in a specific vibrational direction. These approaches can be expanded to 3D vibrations by bonding separate devices into a 3D arrangement which makes this approach expensive, bulky and not capable of being integrated in a planar CMOS process. Additionally, possible misalignment of the components through bonding can reduce the output power of the micro energy harvester. Other electrostatic harvesters using external circuits for biasing or supplying voltage/potential across comb-like capacitors have been reported by Basset et al. (2009) and Nguyen et al. (2010). These architectures suffer the disadvantage of requiring complex circuitry to bias the comb-like capacitor electrodes. The needed circuitry must be powered with batteries (external voltage supply) or from the energy harvested by the harvester with some sort of turn-on from a stand-by battery. In contrast, electret-based energy harvesters allow for miniaturization and monolithical integration of the harvester into a microsystem. Electrets are insulators which have been charged and which can hold these charges for a very long time (several years). Important properties of electrets for energy harvesters are charge density and long term stability of the charges. Charging electrets is done by corona charging (Arakawa et al. 2004) or by ion-implantation (Mescheder et al. 2009). In this paper a new charging method of charging electrets with superior charging and charge stability is discussed. The design and realization of an electret-based vibration energy harvester with integrated components capable of harvesting energy from multi-axial vibration sources by transducing mechanical to electrical energy is presented. A very promising approach to overcome limitations such as pull-in effect which is in conventional designs avoided by bulky spacers between corresponding electrodes (Kiziroglou et al. 2009) is to place the electrets on the vertical sidewalls of comb like electrodes. There is little scientific work on building 3D electret-based vibration energy harvesters with monolithic CMOS processes, the only notable work outside this work is reported by Yamashita Kiyotaka et al. (2010) and Honzumi et al. (2010) using soft X-rays to charge electrets on vertical sidewalls.

2 Design and simulation

2.1 Design

The micro energy harvester was designed to transfer vibrational energy from arbitrary directions to electrical
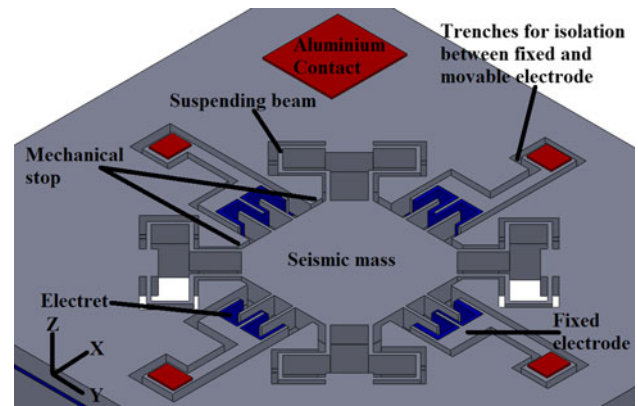

Fig. 1 Design structure of the micro harvester with electret only on sidewalls of fixed (*outer*) comb-like electrodes

energy ("3D harvester"). The harvester is based on a conventional spring-mass-system with incorporated electrets. The distinguished features of this new approach are the specific design of suspending beams, comb electrodes and the placement of electrets (Figs. 1, 2). The folded beams which hold the central seismic mass were designed so that they are orientated at an angle of 45° to the fingers of the comb electrodes. Therefore, the projections to the x- and y-axis of a mechanical energy component acting on the seismic mass and being directed in any arbitrary direction, is distributed to the four comb capacitors. This gives the possibility of equivalent mass movement in x- and y-direction and makes possible out of plane movement (z-direction). The design of the harvester integrates the placement of electrets on the vertical sidewalls of fixed finger electrodes of comb-like capacitors while realizing movable finger electrodes which are directly connected to the seismic mass with no electrets grown on its sidewalls. This allows for a three dimensional (3D) movement of the seismic mass even for a planar design and for a fabrication compatible to standard CMOS processing with all functional structures defined on a single wafer. As a result, the planar system allows taking up vibrational energy out of all directions; x, y and z.

The fabrication of the 3D micro harvester is based on using silicon on insulator (SOI) wafers with the buried oxide (BOX) between the handle layer and the device layer. Thus, the seismic mass is made up of all these three layers and is therefore relatively large on a given area (some mm²). As SiO₂ electret is used, it is grown thermally in-between opposite fingers/combs forming plate capacitors with a higher potential on the fixed electrode (with electrets) with respect to the moving finger electrodes while the mass and the suspending beams form a mechanical network to couple this electrostatic part. The area of the silicon, connected with fixed finger electrode is reduced by etching a trench to the buried oxide around the

Fig. 2 a Picture of the designed harvester; zoomed. **b** View from the rear side of the harvester chip, **c** cross section, the suspending beams are not shown in this cross section
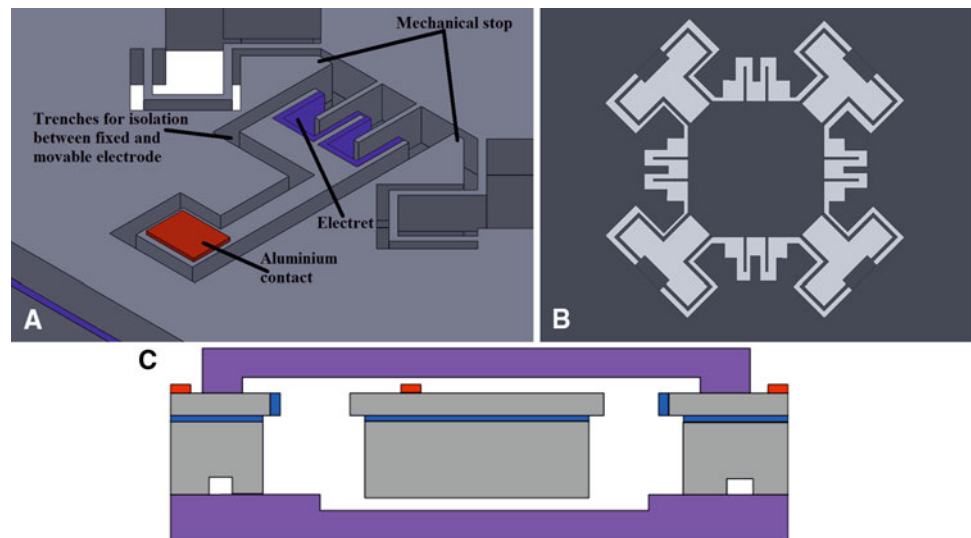

fixed fingers and bond pads so that the parasitic capacitances in the micro-harvester can be reduced (see Fig. 2a). The movement of the mass as a result of external vibrations causes displacement of the finger electrodes and hence capacitance change which drives current/charges out/in the system due to the potential difference between the fixed finger electrodes (with electrets) and the movable finger electrode (without electrets). Pull-in effect is a principle limitation for any energy harvester with capacitive comb-like surfaces due to electrostatic forces. In the presented design the effect of in-plane or in-gap pull-in is avoided by mechanical stops (see Fig. 2a) as protruding arms of the chip frame between the fixed finger electrodes and movable finger electrodes. The stops are mechanically part of the movable electrode/seismic mass of the micro energy harvester. However, they are electrically insulated from the fixed electrodes to avoid discharging the electret charge when contacting the mechanical stops. Figure 2b shows the view from the rear side of the harvester to illustrate which parts of the wafer are totally removed by etching both, the handle layer from the backside and the device layer from the top side (white area), and which parts (trenches for insulation and reduction of parasitic capacitances) are etched into the handle layer only. Whereas the stops for x- and y-direction are realized by suitable structures defined within the device layer of the SOI-wafer, the stops in z-directions are realized by two glass chips (cap and bottom chip) as shown in Fig. 2c.

2.2 FEM simulation

Optimizations of the geometrical parameters were carried out using finite element simulation software COMSOL multiphysics. The design of the 3D harvester was optimized for high output at typical vibration amplitude of 1 g

in all directions at low frequencies (less than about 150 Hz, typically occurring in mobile devices during walking) while preventing pull-in between mass/moving comb-like electrodes and the electrets/fixed comb-like electrode. The simulations were split into mechanical simulation and electrical simulations. A complete 3D model of the 3D harvester was created for both, mechanical and electrical simulations. For mechanical simulations, the model solves the stress and strain as result of 1 g load and predicts deformations of the central seismic mass under frequency sweep of up to 150 Hz. The arbitrary Lagrangian–Eulerian (ALE) method was used to couple deformations and displacements of flexible elements due to relative movement of the seismic mass in respect to the fixed frame to corresponding changes of the electric field and capacitances of the charged electrodes. This accounts for the geometrical changes associated with the deformation. The mechanical simulation provides the magnitude of stress (van Mises) on the total harvester and the seismic mass displacement in x-, y- and z-directions under acceleration (1 g) and frequency (25–150 Hz). This information was used to fix the range of movement of the movable electrode. Stresses as a result of processing; DRIE, handling and packaging were not incorporated in the mechanical simulations. Figure 3 shows the movement of the seismic mass and the corresponding deformation of the suspending beams caused by 1 g vibration in x- or y-direction (Fig. 3a) or z-direction (Fig. 3b). The resulting stress (at 35 Hz) is 37 MPa in-plane and 82 MPa out of plane (z-direction). The resonance frequency for the shown structure is 135 Hz. The beams and the seismic mass were chosen so that the stress also for 1 g vibration in z-direction is less than 100 MPa. Another design criterion is to prohibit pull-in effects and deformation of the movable electrode due to the high electrical field provided by electrets covering the sidewalls
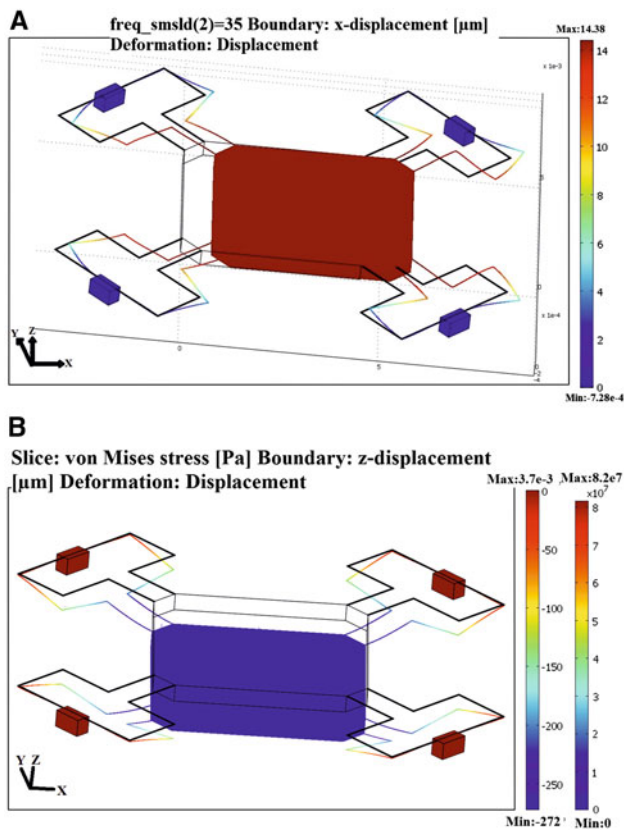
Fig. 3 a Comsol simulations; acceleration of 1 g in X- or Y-direction at 35 Hz. The stress for vibration in X- or Y-direction is 37 MPa at this frequency and 100 MPa in Z-direction. Displacement of 13.4 μm is achieved from x or y load. Resonance occurs at 135 Hz either in X- or Y-direction. **b** 1 g load in z-direction, maximum displacement 272 μm, maximum stress around 82 MPa

of the fixed electrode. Pull-in can arise from two possibilities, first when the vibration of the combs/seismic mass is so large that it brings opposing electrodes together and secondly when successive fingers pull together as a result of electrets based electrostatic forces between them as they get closer to each other through vibration. The first of the two effects is catered for by designing mechanical stops (see Fig. 2a). The second effect which deals with successive fingers getting stuck together due to electrostatic forces between them was cleared with COMSOL to find optimal parameters to prevent pull-in. For geometrical values listed in Table 1, the deflection of the movable electrode due to the electric field by electrets charged with 800 C/m³ (corresponding in this case to a surface charge density σ of 14 mC/m²) is only 149 nm and can be neglected. The corresponding stress in this case is very small (<10 MPa).

The dimensions given in Table 1 were chosen out of the simulations as the optimized design parameters which gave the best displacement/stress ratio under 1 g up to 150 Hz in x- and y-direction and which did not result in pull-in of fingers even at electret potential of up to 450 V.

Table 1 Chosen design specifications of the presented 3D micro harvester concept

| Parameter	Optimized value from FEM simulations
Thickness of mass (μm)	411.00
Length of beam (mm)	1.50
Width of beam (μm)	30.00
Thickness of beam (μm)	10.00
Acceleration (g)	1.00
Width of beam (μm)	13.40
Finger length/breadth (μm)	100/5
Finger gap (μm)	9.50
Allowable vibration distance (μm)	8.50
Electret thickness (μm)	0.50
Potential on the electrets (V)	Up to 400

3 Theoretical output power

Based on Mitcheson et al. (2004), harvesters can be categorized into so-called velocity-damped resonant generators (VDRGs) and Coulomb-damped resonant generators (CDRGs). Mitcheson et al. (2004) proposed a general formula for the output power of such harvesters. For electrostatic harvesters with an external source of voltage (such as presented by Basset et al. 2009 and Nguyen et al. 2010) or different charging mechanism than electrets, Meninger (2001) proposed a cycle of voltage-constraint and charge-constant cycles for the energy conversion. For a harvester with electrets serving as the source of potential which do not change (ideally) with time and under operation of the electrostatic micro harvester, these models may not apply for forecasting the output power. The harvested electrical energy depends strongly on the static voltage of the electrets and the change in capacitance. For the designed 3D electret-based vibration energy harvester (Fig. 1), there are four sets of comb-like structures forming four sets of capacitances. The capacitance of comb-like pair is given by Eq. 2, as a series capacitance of the capacitance $C_{electret}$ provided by the electret charges and the corresponding mirror charges at the two sides of the electret and the variable capacitance C_{air}, formed by the fixed and movable plate like electrodes as shown in Fig. 4 (right).

$$C = \frac{C_{electret} \times C_{air}}{C_{electret} + C_{air}} \tag{2}$$

The displacement x of the mass m relative to the housing (fixed parts of the harvester) is described in Eq. 3, which results in a change of capacitance between the capacitive comb finger electrodes.

$$m\frac{d^2x}{dt^2} + c\frac{dx}{dt} + kx = m\frac{d^2y}{dt^2} \tag{3}$$

Fig. 4 *Left* electrical model of the harvester formed by four capacitances (with two electrode fingers aligned in *x* and two fingers aligned in *y*-direction), *right* the capacitance is given by a series capacitance formed by the negative charges on the electrets surface and the mirror charges at the interfaces electret/Si and by the air filled capacitance between movable and fixed electrode finger
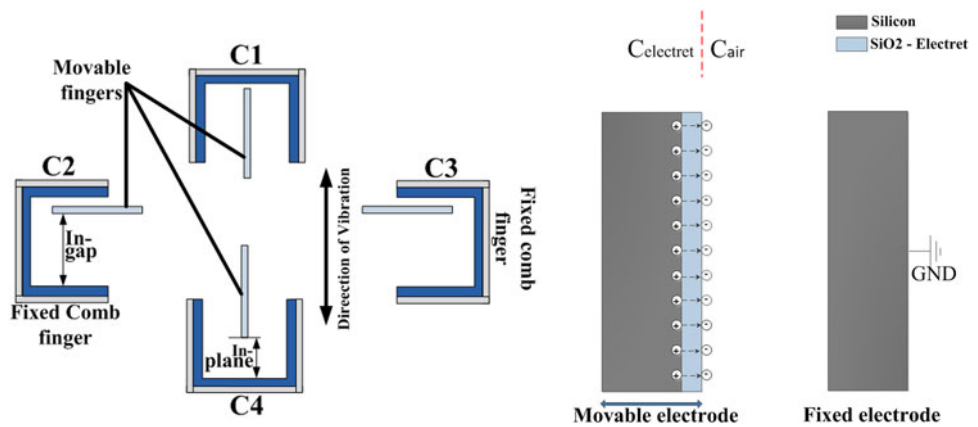
where $m\frac{d^2y}{dt^2}$ is the force provided by an external vibration y of the housing and acting on the seismic mass m, k is the suspending beams stiffness constant and c the damping coefficient due to resistance; e.g. in air. The energy stored on a comb-like finger electrode forming a capacitor is given in Eq. 4. Here, E is the energy stored on a finger pair, V is the electrets potential relative to the moving finger electrode, showing the strong dependence on the achieved electrets potential ($E \sim V^2$). For electrets-based capacitive harvesters, the potential V is related to the surface charge density on the electrets σ (Eq. 5)

$$E = ^1\!/_2(CV^2) \tag{4}$$

$$\sigma = \varepsilon_0 . \varepsilon_{el} . \frac{V}{t_{el}} \tag{5}$$

Ideally, the potential on the electrets does no change after charging and during operation of the harvester; the variable parameter is the capacitance between movable and fixed electrode which is changed by subjecting the housing of the harvester to vibrations. The change in capacitance may not be perfectly sinusoidal and may be a changing function with time, but assuming a perfectly sinusoidal change of capacitance with time, the capacitance can be written as Eq. (6).

$$C = C_o + C_{max} \sin(2\pi ft) \tag{6}$$

By differentiating the energy stored on the total fingers/capacitances with respect to time and assuming the change in capacitance is perfectly sinusoidal, the output power of an electrets-based vibration harvester with capacitive comb-like fingers/surfaces can be predicted based on Eq. (7):

$$\frac{\partial E}{\partial t} = \frac{V^2}{2}\left[\frac{\partial(C_o + C_{max}\sin(2\pi ft)}{\partial t}\right] \tag{7}$$

The power P is then

$$P = \frac{V^2}{2}\left(C_{max}2\pi f \cos(2\pi ft)\right) \tag{8}$$

where C_{max} is the maximum capacitance between cumulative comb-like fingers and C_o is the mean capacitance of cumulative comb-like fingers. The maximum possible power will be harvested when $\cos(2\pi ft) = 1$. For the geometries given in Table 1, an assumed electret potential of 250 V and vibration of 1 g (walking), the calculated maximum power of the device is 10 μW.

4 3D harvester fabrication process

Silicon on insulator-wafers were used to provide a relative simple fabrication process to create movable elements (springs, electrodes, seismic mass) with high precision (especially thickness control). A 400 μm handle layer, a 2 μm BOX and a 10 μm device layer was chosen to realize the dimensions listed in Table 1. The fabrication process of the 3D electrets based vibration energy harvester involves a MEMS process compatible with standard CMOS processing and materials. It uses deep reactive-ion etching for anisotropic etching of silicon for releasing the seismic mass, capacitive finger electrodes and suspending beams, and local oxidation using Si_3N_4 as passivation to grow thermal oxide on the sidewall of the fingers electrodes only. This grown SiO_2 (later charged to form the electrets) is selectively etched in BHF with photoresist mask to leave the SiO_2 only on the sidewalls of the fixed electrode fingers. Sidewall etching of the moving finger electrets is necessary due to the special charging technique presented in Sect. 5 which provides only charging with one polarity (negative ions). In this case a biasing potential between fixed and movable electrode would be needed to create a suitable potential difference between these electrodes if both are covered with electrets. To be independent on biasing during charging, only the fixed electrode should be

Fig. 5 Microscopic images of electret structuring process (*top views*) **a** photolithography in 10 μm deep structures to etch opposite finger oxide (electret), photo resist covering one side of finger only, **b** after BHF etching and resist removal: electrode width without electret 5.7 μm, electrode width with electret 6.8 μm, calculated electret thickness: 0.55 μm
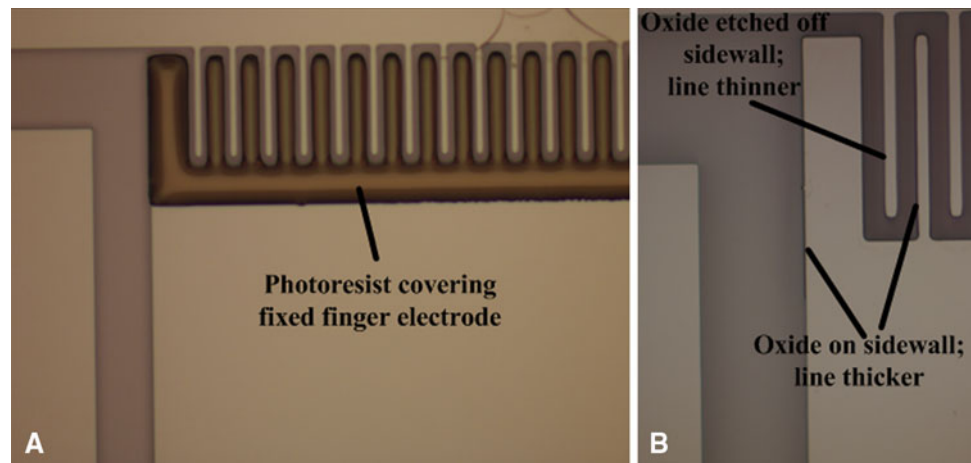
Fig. 6 Fabricated 3D electrostatic energy harvester. *Left* processed SOI-chip, *right*: packaged chip between two glass wafers acting as mechanical stops in Z-direction
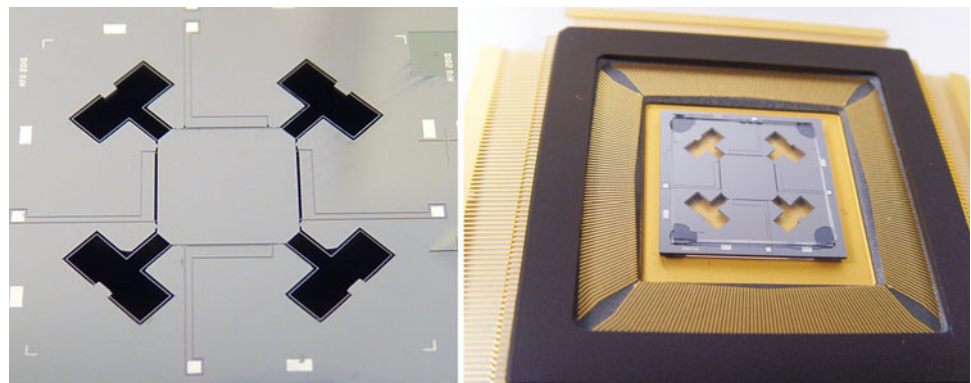
covered with electrets. Figure 5 shows the microscopic picture of this specific process step which requires a photo process on the 10 μm deep electrode structure. As can be seen on the right hand side of Fig. 5, the process works well.

Five lithography masks are needed to structure the SOI-wafer. Two masks are needed to structure the protecting glass chips which act as stops for *z*-direction movements of the seismic mass. A defined gap of 5 μm on both sides of the glass substrate is etched for this purpose (Fig. 2c). The glass is wet etched using poly-Si as masking layer. Details of the fabrication process are presented in (Nimo and Mescheder 2010). Figure 6 shows a structured harvester chip and the total device after bonding the glass chips to the SOI-chip. Due to the high sensitivity of the structure (1 g to all directions) very careful handling of the device after release of the movable structures and before bonding is essential to avoid disintegration of the very sensitive structures. Especially in *z*-direction, the free displacement of the seismic mass by around 270 μm under 1 g load (which is also the static offset by the earth's gravitational force without the stops provided after the bonding to the glass wafers) has to be avoided by special measures during transportation and handling.

5 Charging electrets with hair-dryer

The performance of a capacitive, electret based micro harvester is mainly determined by the charge density σ of the electret (Eq. 5). Other important material properties are long term stability of charges on electrets and temperature stability. For the design presented in Sect. 2, the capability to charge electrets on vertical sidewalls has to be considered. In this section a simple electret charging technique using ionic hair-dryer is presented. First the charging of planar electrets as used in conventional designs is discussed. Then the specific results of charging electrets on vertical sidewalls are presented.

5.1 Electret sample preparations and charging set-up

SiO$_2$ and CYTOP were investigated. The material properties of SiO$_2$ and CYTOP which are important for use as electrets are listed in Mescheder et al. (2009). Standard 10–15 Ω cm boron doped (100) 4″ Si-wafers were used for these experiments. SiO$_2$ was thermally grown on both sides of the silicon wafers with different thicknesses (0.5–1.5 μm). CYTOP was spin coated to different thicknesses (5–10 μm).

Details of the sample preparation and the charging setup are presented in Saad et al. (2010). Instead of the well known corona charging (Arakawa et al. 2004) or ion-implantation (Mescheder et al. 2009), a low cost charging method using commercial so-called ionic hairdryer (Braun model 3549) was used. In this type of hairdryers, ions are produced to compensate for charging of hairs e.g. by combing. A ground contact of the wafer backside is important to get good charging results. Oxide or aluminum coated on the backside of the chips to be charged did not affect the electrostatic potential measured on the charged electrets frontside. The electret surface to be charged was arranged perpendicularly, parallel or at arbitrary angles with respect to the ionic air flow from hairdryer. After charging the electrets, the surface potential was measured with an electrostatic voltmeter (Model 541-1, TREK, USA; measurement accuracy ±10 V).

5.2 Results of charging electrets samples

Using the ionic hairdryer; Braun 3549, charging time of 30 min was sufficient for obtaining the maximum possible potential of 1,000 V on a planar electret layer. 1,000 V is the measurement limit of the electrostatic voltmeter 541-1 from TREK. The surface potential increases with charging time until about 30 min, reaching a saturation potential proportional to the thickness of the electret. Within the tested distances between electrets surface and ionic hairdryer outlet (ranging from 12 to 110 mm), the achieved surface potential on the electrets did not change significantly (difference of less than 12%). The average air speed from the ionic-hair dryer was around 7 m/s, (measured with thermal anemometer TESTO 425). Due to the sharp tip of the ion source in ionic hairdryers and non-uniform ionic air flow, uniformity of charge potential over a 4″-wafer is normally poor. However, by grounding the sample backside and rotating the samples during charging, a reasonable homogeneity of surface potential on 4″ wafers was achieved (±16%). These general results were presented in (Saad et al. 2010).

5.2.1 Long term stability of electret charge

The long term stability of charge on electret is essential for any electret-based vibration energy harvester. Electret potential was checked within three time periods: short term (hours–some days), medium term (10–50 days) and long term (>100 days). Figure 7 shows that the surface potential charged by ionic hairdryer for both SiO_2 and CYTOP are very stable in time compared to corona charging or charging by ion-implantation (Mescheder et al. 2009). For SiO_2, a relatively small decay of charged potential does occur (after more than a year around 20–30% loss of initial value). The decay does not depend significantly on the starting electret potential
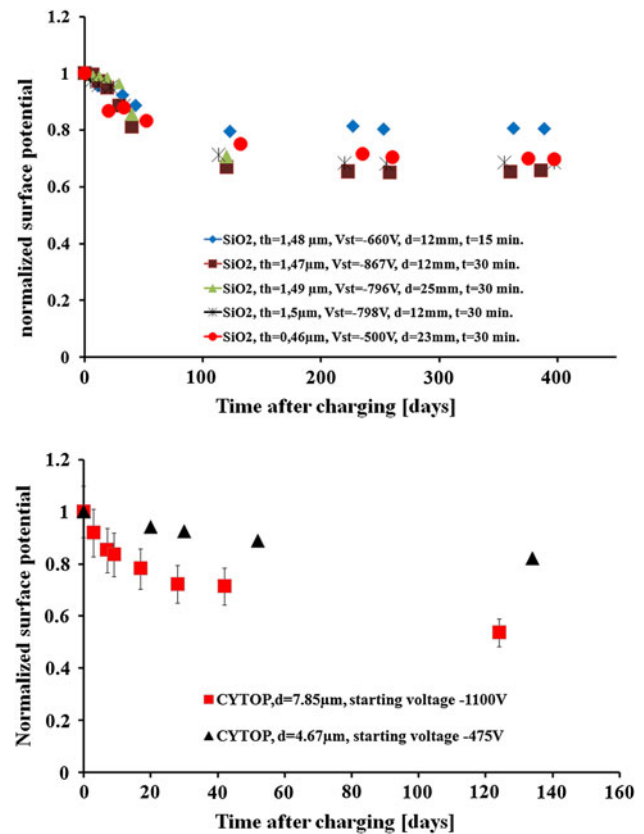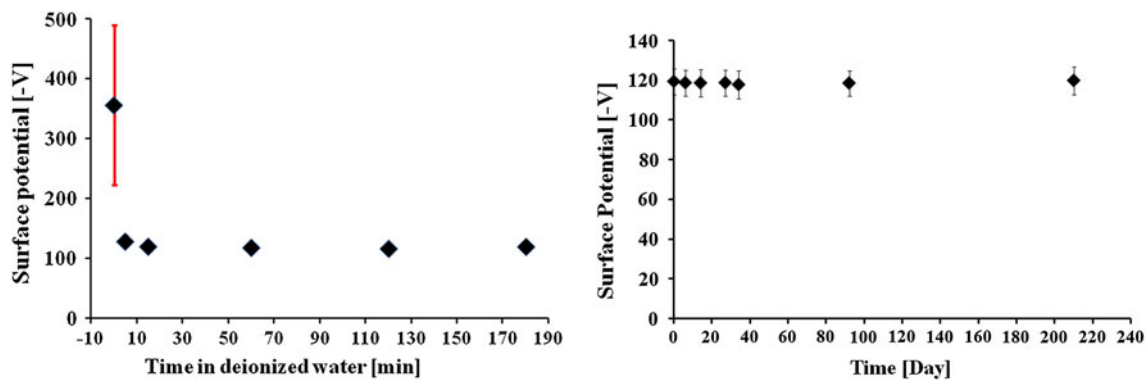

Fig. 7 Long term stability of charges in electrets charged with ionic hair dryers for SiO_2 (*top*), and for CYTOP (*bottom*). The potential is normalized to the starting potential (max. value) directly after charging. *Error bars* indicating typical errors due to local potential variation

(ranging from 500 to 867 V) within the first 30 days. For long term decay (after about 100 days), only for the electret with lower ratio of initial (starting) charged potential (V_{st}) to electrets thickness d_{el} ($V_{st}/d_{el} = 445$ V/μm) a slightly smaller decay was observed than for those electrets with larger V_{st}/d_{el} ratio (534, 589 and 1,086 V/μm). For CYTOP, a significant dependence of charging loss on V_{st}/d_{el} ratio is observed, both, for medium and long term measurements. The relative loss of potential is only 20% for low V_{st}/d_{el}-ratio ($V_{st}/d_{el} = 102$ V/μm) whereas the loss is almost 50% for $V_{st}/d_{el} = 140$ V/μm. It is obvious that the charging performance of SiO_2 is better than that of CYTOP since for a given electret thickness the achievable electret potential is up to ten times larger for SiO_2 than for CYTOP.

5.2.2 Stability of electret charge in moisture

The stability of charges in moisture has to be considered during manufacturing if the electret charging step is not the final processing step (e.g. dipping into water for cleaning after charging). Additionally, for practical use it is important to know if a watertight package is needed during operation.

Fig. 8 *Left* charge resilience due to rinsing 7.8 μm CYTOP charged electret in de-ionized water. *Right* long term stability of charges in CYTOP after rinsing in de-ionized water for 180 min. The *error bars* are the standard deviation over the CYTOP layer on the 4 inch silicon wafer which is about 20× smaller after rinsing than before rinsing

The stability of the charge on the electrets was investigated in extreme conditions such as moisture and rinsing in de-ionized water for both, SiO$_2$ and CYTOP. Figure 8 shows the charge resilience (charged with ionic hair dryer) of CYTOP after rinsing in de-ionized water. The CYTOP electret initially charged was dipped in de-ionized water for up to 180 min. The surface potential dropped from −356 to −128 V within 5 min rinsing in water and remained stable at −120 ± 7 V from 15 to 180 min in water (each measurement after dipping and drying with dry nitrogen). As can be seen in Fig. 8 left, by rinsing charged CYTOP in de-ionized water, the uniformity of charge density over the wafer surface is considerably improved to ±10% as indicated by the error bars. Whereas the spread of the electret potential over the 4″-wafer is ±133 V before rinsing, the potential is very uniform after rinsing (±7 V only). Additionally, rinsing improves the long term stability of the CYTOP electrets (Fig. 8 right). However, the maximum charge density is reduced by this procedure (Fig. 8 left) so that the potential to thickness relation is reduced to V/d$_{el}$ = 15 V/μm, which is much less than before rinsing (V/d$_{el}$ = 46 V/μm). In sharp contrast, the charges in SiO$_2$ electret did not survive rinsing the samples in de-ionized water: the charges disappear immediately after rinsing. This means charging should be done at the end of a manufacturing process before packaging, especially when SiO$_2$ electret is been used. For applications requiring good homogeneity or good long term stability of charge density, a pretreatment of CYTOP by rinsing may be used to remove unstable charges from the surface.

5.2.3 Temperature stability of charged electret samples

Charge stability under high temperatures is investigated to characterize the range at which the 3D micro harvester can work without degeneration when charged with the ionic hair dryer technique. Obviously the most sensitive component in any electret-based vibration energy harvesters to
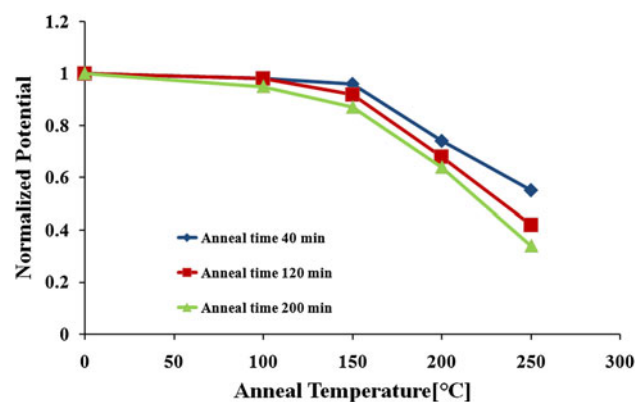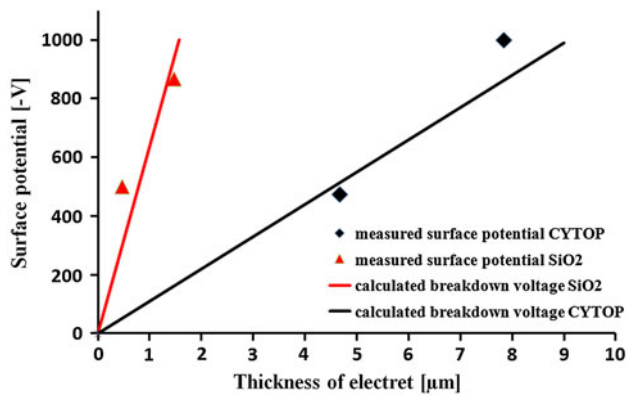

Fig. 9 Temperature stability of charge on SiO$_2$ surface. The potentials have been normalized to the electret starting potential on each of the wafers. SiO$_2$ thickness $d = 1.3$ μm, charging time 30 min

temperature is the charge density of the electret. Figure 9 shows the decay of SiO$_2$ electret surface potential under temperature treatment. Samples were treated at specific temperatures ranging from 100 to 250°C for 40, 120 and 200 min cumulative. The process is repeated by increasing the temperatures starting from 100°C at intervals of 50°C of up to 250°C. The samples were cooled down to room temperature before measuring the surface potential. The potential on SiO$_2$ electret charged with ionic hairdryer are stable to temperature increase up to about 150°C. The additional influence of annealing time is relatively small: at 250°C, a cumulative anneal time of 200 min decreases the normalized surface potential slightly from 60% (anneal time 40 min) to 40% (anneal time 200 min).

5.2.4 Dependence of charge density on thickness of electrets layer

The charge density σ is related to the surface potential V and electrets thickness d_{el} by Eq. 5. Figure 10 shows measured values of maximum electret potential charged by
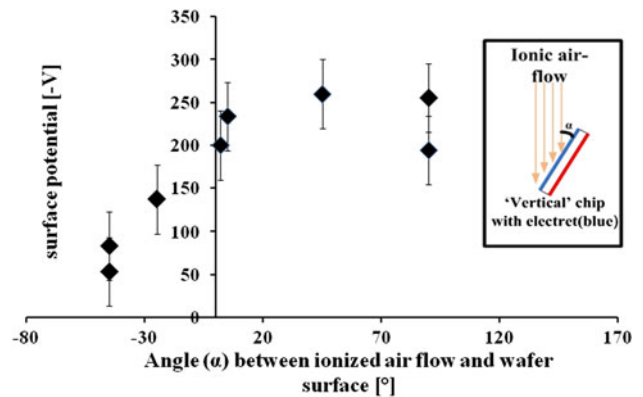
Fig. 10 Dependence of achieved surface potential on electrets thickness

Fig. 11 Surface potential of electret (here SiO$_2$) versus angle α between air flow from hairdryer and electret surface. Insertion: chips of 1 cm × 2 cm were charged, 0.58 μm-thick SiO$_2$ electret on front side (*left side*) and grounded aluminum on backside (*right side*). The negative *x*-axis indicates a situation where air flow hit the backside, but still front-side is measured

ionic hairdryer for different thicknesses of the electrets for both, SiO$_2$ and CYTOP. Typically, thermally grown SiO$_2$ will breakdown at electrical fields between 800 and 1,100 V/μm. This means the breakdown voltage for a 0.5 μm thermally grown oxide should be between 400 and 550 V. This corresponds well to the experimental results shown in Fig. 10 demonstrating the good quality of the used SiO$_2$. For CYTOP the achieved values correspond to the breakdown voltage of 110 V/μm as reported by Asahi (Asahi Glass Co Ltd. electrical data table CYTOP. http://www.agc.com/english/chemicals/shinsei/cytop/electric.html). The ionic hairdryer method resulted in excellent surface potential of more than −1,000 V when charging 7.8 μm CYTOP and 1.5 μm SiO$_2$ electret films placed perpendicular to the flow of ionic air (Saad et al. 2010). Using Eq. (5), the charge density σ can be calculated as 37.5 mC/m^2 for SiO$_2$ (potential of −500 V for 0.46 μm SiO$_2$) and 2.4 mC/m^2 for CYTOP (measured surface potentials of −1,000 V for 7.84 μm CYTOP). These values are the highest reported values for CYTOP and in the case of SiO$_2$ two times higher than the highest reported values so far (Zhang et al. 2007). The achieved value for SiO$_2$ is even larger than for Teflon where the largest σ of all electret materials has been reported so far (Boland et al. 2003).

5.2.5 Charging electrets on sidewalls

Until now, the results discussed were achieved by placing the electrets' (SiO$_2$ or CYTOP) surface perpendicular to the flow of ionic air from the ionic hairdryer. This is important for the general characterization of the charged electrets for applications in micro energy harvesting or other applications. But for the specific use of electrets for 3D energy harvesting presented in Sect. 2, a charging process capable of charging electrets deposited on vertical sidewalls (surfaces 'parallel' to the flow of ionic air) is necessary. This cannot be achieved with corona charging

due to the high energy of the ions and thus well defined direction of accelerated charges. Charging electrets on sidewalls of finished devices with ion implantation is also not possible and will potentially damage fragile components and possibly change the doping profile of the substrates which may change the behavior of the micro-energy harvester. Recently, Honzumi et al. (2010) presented soft X-ray charging for electrets on vertical sidewalls. By using an ionic hair-dryer to charge these electrets, a simpler approach is proposed. Figure 11 shows the dependence of surface potential on the angle α between air flow and surface of the electrets. The measurements were done on single chips (chip area 1 × 2 cm^2). The surface potential depends only slightly on the specific angle α between the ionic air flow and the surface of the electrets so far as α is positive. For negative α (air flow hitting wafer backside) the surface potential on the electrets decreases considerably. These results prove the principle feasibility of this charging technique for charging electrets on vertical sidewalls.

However, charging electrets on vertical surfaces (fingers) of parallel plates resulted in a considerable drop in surface potential at distances less or equal to about 2 mm (Fig. 12). The results shown in Fig. 12 were obtained for a large aspect ratio of plate's depth (3–10 mm) to distance of plates (0.1–5 mm). It was possible to double the potential on narrow separated electrodes by longer charging; but the increase was considerably lower than estimated for a linear dependence on charging time. Additionally, suitable grounding of the back-surface of the capacitive surfaces is needed: letting the backside of charged surface float resulted in zero potential even at a reasonable large electrode separations of 0.5 mm. It was observed that for very small gaps, the surface potential was not constant along the

Fig. 12 Dependence of surface potential on distance d between two parallel plates covered with SiO₂-electret after charging sidewalls with ionic hair-dryer (SiO₂ on front sides positioned oppositely to each other; Al on backside; temperature of charging 38°), curve: polynominal fit for 3 × 20 mm² large plate
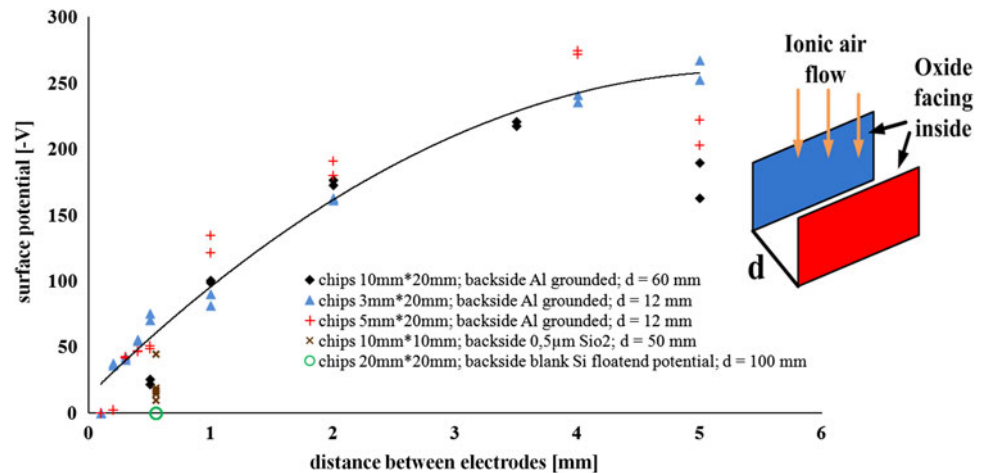
depth (direction of air flow) of the two parallel chips: smaller potential were observed at the bottom of the electrodes than at the top. In the design presented in Sect. 2, the depth of the comb electrodes is only 10 μm. So larger values of surface potential may be expected, but cannot be measured directly due to the limited spatial resolution of the electrometer (averaging on an area of around 1 mm²).

6 Discussion

The most important issue for the presented 3D energy harvester with electret deposited on the vertical sidewalls of comb like parallel plate capacitors is the ability to charge the electret with reasonable large potential. Therefore, the measured charging performance of the new low cost charging principle is discussed. For this purpose the energy of charged and not charged molecules in the airflow of an ionic hairdryer is first analyzed. As the charge creation in an ionic hairdryer is similar to that of corona charging, it is assumed that the charging molecules are mainly CO_3^- ions and the surrounding non-charged molecules in air are mostly N_2 molecules. The average kinetic energy of N_2-molecules (Maxwell distribution) at T = 300 K is around E_{kin} (N_2) = 3×10^{-2} eV and the corresponding mean value of the molecular velocity is 450 m/s. The air velocity of the used hair dryer has been measured with a thermal anemometer (Testo 425) as 7 ± 1 m/s (free flow). With a 4″-wafer perpendicular and close to the outlet of the hair dryer, the air velocity is only 2 m/s in the center and around 10 m/s at the periphery of the wafer. Therefore, the hairdryer's directed air flow in any case is much smaller than the arbitrarily directed Maxwell velocity. This explains the good charging of sidewalls which are directed parallel to the air flow of the

hairdryer (Fig. 11). The smaller values for the maximal potential even in horizontal position (α = 90°) as shown in Fig. 11 and compared to previous results obtained on wafers is attributed to the non-uniformity of ion concentration within the air stream of an ionic hair dryer and the lower dynamic pressure created by a small chip compared to a 4″-wafer. Thus, the interaction time for the ions in the air flow and therefore the probability to being attached to the surface is larger when charging large wafers than for charging small chip areas. The large potential achieved by this technique for electret placed perpendicular to the air flow (Fig. 10) can be explained by a simple model. The electric field above an infinite plate uniformly charged with a charge density σ = 37.5 mC/m² is (air: ε_r = 1).

$$E = \frac{\sigma}{2\varepsilon_0\varepsilon_r} = \text{const} = 2,087 \ V/m \tag{9}$$

Therefore, on a new CO_3^- ion appearing at such a charged surface an electrostatic force of only 3.34×10^{-10} N will act. Considering a free path length between collisions of s = 68 nm (value for N_2 at 300 K and 1 bar) and a molecular weight M(CO_3) = 1×10^{-25} kg, the maximum velocity v_{el} of this ion due to the acceleration in the electric field of the already charged plate (directed away from the plate) and taken up between two collisions can be calculated:

$$v_{el} = \sqrt{\frac{2e\sigma s}{2M\varepsilon_0\varepsilon_r}} = 21.1 m/s \tag{10}$$

where $e = 1.6 \times 10^{-19}$ C (single charged ion).

Comparing this velocity provided by the repellent forces of the charged plate to the arbitrarily directed thermal velocity (450 m/s for N_2 and around 210 m/s for CO_3^- due to momentum transfer from N_2 by collision), it is obvious that the thermal velocity is large enough to overcome the repellent force provided by the already charged plate even for very large potentials or charge density (1,000 V or 37.5 mC/m²). Therefore, the charge density is limited in

this case only by the breakthrough voltage which is increasing with increasing thickness of the electret as can be seen in Fig. 10. However, comparing the achieved maximum potential or charge density to that achieved by standard corona charging or ion implantation (Mescheder et al. 2009) it can be concluded that charging with an ionic hair dryer is superior. E.g. the maximum reported potential achieved by ion-implantation of 0.5 μm thick SiO_2 was only 230 V, which is less than half the value obtained with an ionic hair dryer. This behavior is attributed to the low energy of the charging ions of hair dryer and the creation of defects by high energy bombardment in the case of ion implantation or corona charging. The small force impact of the charging ions on the SiO_2 electret might also be responsible for the better long term stability of ions charged with ionic hair dryer (Fig. 7) compared to ions charged with corona charging or ion implantation (Mescheder et al. 2009).

On the other hand, charging of parallel plates in close distance is limited even with an ionic hair dryer as shown in Fig. 12, even though single vertical plates can be charged very well. To understand this limitation, an air flow in a small rectangular channel (slit) is considered. Assuming a laminar flow, the Hagen-Poiseuille relation (Eq. 11) gives an average velocity of air provided by a blower of a typical hair dryer within the slit

$$\overline{V_{flow}} = h^2 \Delta p / 12l\eta \tag{11}$$

where h is the gap between the plates (channel height), l the channel length (height of the plate), η the viscosity of air and Δp the dynamic pressure provided by the blower. With

$h = 0.1$ mm, $\Delta p = 30$ Pa, $l = 3$ mm and $\eta = 17.4 \times 10^{-6}$ Pa s an average velocity within the slit of about 0.5 m/s is expected which is somewhat smaller than the measured air flow velocity in a free flow or directed on a wafer, but large enough for sufficient supply of ions even in small electrode gaps as seen in Fig. 12.

However, for further reduction of h to some microns, the flow velocity will become a limiting factor for charging parallel plates. The relatively low air flow might also cause the observed slight dependence of surface potential on distance to the slit entrance (top of the parallel plates), showing a decrease by about 30% for an extremely large height of 1 cm. The most important difference between charging an isolated single plate and a vertical parallel plate capacitor is the difference in the repelling forces acting on an appearing negatively charged ion by the already built up negative potential on the plates. This difference is schematically presented in Fig. 13. In the case of a single (infinite large) plate the constant electric field calculated for the charge density σ using Eq. 9 is about 2,087 V/m and the repelling electric force relatively small. However, the situation is very different for two parallel plates in close distance and placed parallel to the air flow, in this case the stray field at the top end of the plates formed between the already charged electret surface (negative) and the mirror charges (positive) (Fig. 13 right) is very large. Even at potentials as low as −20 V, the electric field within the electret (thickness 0.5 μm) is 10^7 V/m. Hence the stray field in air is several orders of magnitude larger than the repelling electric field in the case of a single plate charged up to −1,000 V. This explains
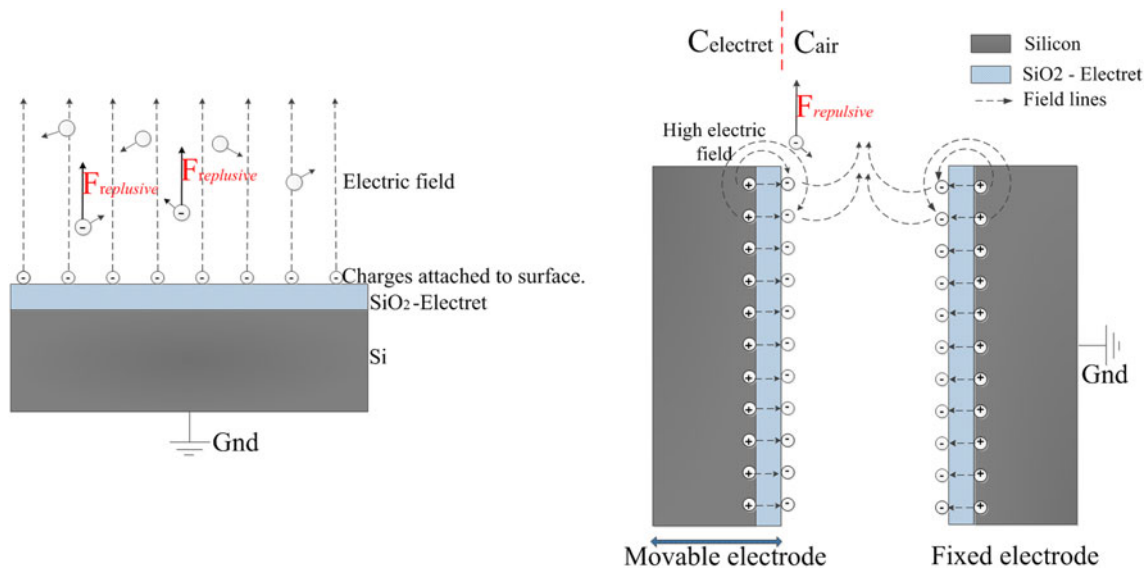
Fig. 13 Model to explain the difference of charging a single plate (*left*) and the inner surface of vertically placed parallel plates (*right*). The *arrows* at the molecules indicate the arbitrarily directed movement due to the thermal energy of the molecules (Maxwell distribution) and the repelling electrostatic force provided by the already charged plates

also why no big difference has been measured for parallel plates where SiO$_2$ electret is deposited on one side (layout used in the 3D energy harvester presented in Sect. 2.1) and parallel plates where the electret is placed on the inner surface of both plates: The electrical field between the plates depends on the plates distance, but is much smaller than the electric field obtained between the two surfaces of the very thin electret (forming a capacitor due to the mirror charge). In this case the velocity which an ion can take up during the mean path length of $s = 68$ nm when being accelerated electrostatically away from the charged plate is approximated as in equation

$$v_{el} = \sqrt{2esE/M} = 1,475 \ m/s \qquad (12)$$

The repelling electric field E is assumed as $E = 10^7$ V/m which is reasonable for a stray field in air near the edge of the capacitor formed by the charged electrets (electric field of $E = 10^7$ V/m in dielectric medium). Obviously, only the ions having higher Maxwell distribution thermal velocity than v_{el} can reach the already charged surface and move into the small slit. Based on this model, the charge density of parallel plates (smaller d) can be increased considerably by an appropriate positive bias potential applied to the outer surface of the electrode plates.

The only significant disadvantage of using SiO$_2$ as electret is its sensitivity to rinsing, whereas for CYTOP 30% of the charges survived rinsing in de-ionized water. The better performance of CYTOP is attributed to the superhydrophobic property of the amorphous fluoropolymer CYTOP and a better charge transfer of surface charges into the layer near the surface where the charge is protected.

Based on the limitations of charging electrets deposited on vertical sidewall of a parallel plate capacitor, the maximum output power of the device presented in Sect. 2.1 and discussed in Sect. 3 is expected to be only 0.1 µW but can be improved to about 1.6 µW by increasing the charged potential to about -100 V by improvements during charging discussed above. Microwatt range of power is the lower limit for practical applications of control electronics.

A severe disadvantage of the presented design is its mechanical sensitivity in z-direction: the very large displacement of the seismic mass in z-direction under a load of 1 g (statically by gravitational force) resulted in a low yield of the fabrication process as the opposite fingers of the comb-like capacitors (fixed and movable electrodes) are moving apart after the release etching process and have to be brought back to the starting position exactly in the correct lateral position ("in-gap") during the bonding process of the bottom chip to the harvester chip. This is almost impossible without breaking at least some of the very fragile finger electrodes.

7 Conclusion

We presented a monolithic design approach for 3D electrets-based micro-energy harvesting. The device is fabricated using SOI-wafers and CMOS compatible processes. Thermal grown SiO$_2$ is used as electret. The device is based on a novel way of developing electrets on the sidewalls of fixed electrodes of the harvester and it achieves 3D vibrational movement by suspending diagonal beams attached to a seismic mass at the center of the micro energy harvester. By this way, vibrational energy from multiple directions can be harvested into electricity. Within our method, the electrets are charged using a method that employs commercially available ionic hairdryers. With the low cost ionic hairdryer, charge densities of 37.5 mC/m^2 for SiO$_2$ and 2.4 mC/m^2 for CYTOP had been measured on single horizontal oriented plates. In the case of CYTP, this value is the highest reported. The obtained charge density for SiO$_2$ is more than twice, the highest ever reported value for an electret. For charging comb-like finger electrets on sidewalls of parallel plate capacitors, the charging performance is considerable smaller. It has been shown that the decrease of charged potential is related to the high repelling electric field occurring at the entrance slit of the parallel plate capacitor. This limitation can be overcome by applying a suitable bias potential during charging. A typical output power of some microwatt is expected for vibrational energy of 1 g acceleration amplitude and less than 150 Hz.

To improve the yield, the sensitivity in z-direction has to be decreased. This is achieved e.g. by using a device layer thickness of 15 µm (thickness of the beams and electrodes) and reducing the length of the beams to about 1 mm and the beam with to about 7 µm. For these geometries the sensitivity in x- and y-direction is only slightly reduced, however the displacement in z-direction is decreased to less than 10 µm ensuring a suitable overlap of the electrode fingers under static load of 1 g. Experimental results of this approach will be published in another paper.

References

Arakawa Y, Suzuki Y, Kasaki N (2004) Micro Seismic power generator using electrets polymer film. Power MEMS 2004, Kyoto, Japan, pp 187–190

Basset P, Galayko D, Paracha AM, Marty F, Dudka A, Bourouina T (2009) A batch-fabricated and electret-free silicon electrostatic vibration energy harvester. J Micromech Microeng 19(11):115025. doi:10.1088/0960-1317/19/11/115025

Boland J, Chao Y, Suzuki Y, Tai Y (2003) Micro Electret Power generator. IEEE 2003:538–541

Edamoto M, Suzuki Y, Kasagi N, Kashiwagi K, Morizawa Y, Yokoyama T, Seki T, Oba M (2009) Low-resonant-frequency micro electret generator for energy harvesting application. Proceedings of the IEEE International Conference on MEMS, pp 1059–1062

Honzumi M, Ueno A, Hagiwara K, Suzuki Y, Tajima T, Kasagi N (2010) Soft-X-ray-charged vertical electrets and its application to electrostatic transducers. Proceedings of MEMS 2010, Hongkong, pp 635–638

Kiziroglou ME, He CR, Yeatman EM (2009) Rolling rod electrostatic microgenerator. IEEE Trans Ind Electron 56(4):1101–1108. doi: 10.1109/TIE.2008.2004381

Mescheder U, Urbanovic P, Müller B, Baborie S (2009) Properties of SiO_2 electret films charged by ion implantation for MEMS-based energy harvesting systems. J Micromech Microeng 19(9):094003. doi:10.1088/0960-1317/19/9/094003

Mitcheson PD, Green TC, Yeatman EM, Holmes AS (2004) Architectures for vibration-driven micropower generators. J Microelectromech Syst 13(3):429–440. doi:10.1109/JMEMS.2004.830151

Nguyen DS, Halvorsen E, Jensen GU, Vogl A (2010) Fabrication and characterization of a wideband MEMS energy harvester utilizing nonlinear springs. J Micromech Microeng 20(12):125009. doi: 10.1088/0960-1317/20/12/125009

Nimo A, Mescheder U (2010) 3D capacitive vibrational harvester for autonomous lowpower sensors. Proc Power MEMS 2010. Poster paper, pp 49–52

Saad A, Mescheder U, Müller B, Nimo A (2010) High-efficient, low-cost electret charging set-up for MEMS-based energy harvesting systems. Proc Power MEMS 2010. Poster paper, pp 61–64

Scott Meninger, Oscar Mur-Miranda Jose, Rajeevan Amirtharajah, Chandrakasan Anantha P, Lang Jeffrey H (2001) Vibration-to-electric energy conversion. IEEE VLSI Syst 9(1):64–75

Tsutsumino T, Suzuki Y, Kasagi N, Sakane Y, and Suzuki Yuji (2006) Seismic power generator using high-performance polymer electret. Proceedings of the IEEE International Conference on MEMS, pp 98–101

Williams CB, Yates RB (1996) Analysis of a micro-electric generator for microsystems. Sensors and Actuator A 52:8–11

Yamashita Kiyotaka, Honzumi Makoto, Hagiwara Kei, Iguchi Yoshinori, Suzuki Yuji (2010) Vibration-driven MEMS energy harvester with vertical electrets. Proc PowerMEMS 2010. Oral paper, pp 165–168

Zhang J, Chen Z, Hao Y, Wen Z, Jin Y, Wen Zhiyu (2007) PECVD SiO2/Si3N4 double layers electrets for application in MEMS power generator. PowerMEMS 2007, Germany, Freiburg, pp 105–108